# Biphasic Electron Transfer Arising from Two Non-Interacting Donating States Unambiguously Revealed in C343-Sensitized Mesoporous SnO2 by Combining Two Complementary Time-Resolved Spectroscopy Techniques

Miguel Ángel Pulido-Lendínez, Marco Ballabio, Andrés Burgos-Caminal, María E. Corrales, Sergio Revuelta, Saül Garcia-Orrit, Víctor Vega-Mayoral, Juan Cabanillas-González, Luis Bañares, Wojciech Gawelda, and Enrique Cánovas

# Biphasic Electron Transfer Arising From Two Non-Interacting Donating States Unambiguously Revealed in C343 Sensitized Mesoporous $SnO_2$ by Combining Two Complementary Time-Resolved Spectroscopy Techniques

Miguel Ángel Pulido-Lendínez[1], Marco Ballabio[1], Andrés Burgos-Caminal[1,2], María E. Corrales[2,3], Sergio Revuelta[1], Saül Garcia-Orrit[1], Víctor Vega-Mayoral[1], Juan Cabanillas-González[1], Luis Bañares[1,4-5], Wojciech Gawelda[1,2] and Enrique Cánovas[1,*]

[1] *Instituto Madrileño de Estudios Avanzados en Nanociencia (IMDEA Nanociencia), Calle Faraday 9, 28049 Madrid, Spain.*

[2] *Departamento de Química, Facultad de Ciencias, Universidad Autónoma de Madrid, Calle Francisco Tomás y Valiente 7, 28049 Madrid, Spain.*

[3] *Departamento de Química Física Aplicada, Facultad de Ciencias, Universidad Autónoma de Madrid, Calle Francisco Tomás y Valiente 9, 28049 Madrid, Spain*

[4] *Departamento de Química Física and Center for Ultrafast Lasers (CLUR), Facultad de Ciencias Químicas, Universidad Complutense de Madrid, Plaza de las Ciencias 2, 28040 Madrid, Spain.*

[5] *Center for Ultrafast Lasers (CLUR), Facultad de Ciencias Químicas, Universidad Complutense de Madrid, Plaza de las Ciencias 2, 28040 Madrid, Spain.*

* *E-mail:* enrique.canovas@imdea.org

**ABSTRACT**

Dye-sensitized metal oxide (dye-MO) mesoporous films are promising building-blocks in the field of solar energy conversion. At the dye-MO interface, the kinetic competition between donor-to-acceptor electron transfer (ET), and other recombination and relaxation channels, largely determines the efficiency in photocatalytic and photovoltaic devices. Since the signals arising from an ET process and those linked with detrimental kinetical deactivation channels in conventional time-resolved spectroscopy techniques have often the same exponential fingerprint, it is still challenging to unambiguously characterize ET lifetimes on these architectures. Following previous works on sensitized oxides architectures, we show that by combining the information gathered in a sample when employing two complementary pump-probe methods, one sensitive to the photo excited electron depopulation in the dye donor, and another sensitive to the photo induced electron population in the MO acceptor, it is possible to remove any ambiguity in the determination of the ET rates in a dye-MO system. Specifically, we have employed Fluorescence Up-Conversion Spectroscopy and Time-Resolved Terahertz Spectroscopy in a Coumarin 343-Tin Oxide (C343-$SnO_2$) mesoporous film to unambiguously resolve two independent non-interacting ET channels with characteristic ET rates and relative amplitudes almost quantitatively matching within error. Our approach stress the potential of combining complementary spectroscopy techniques as a reliable procedure for the characterization of ET in sensitized systems and hence might contribute to the development of improved efficiencies in optoelectronic devices.

**Keywords:** Dye-Sensitized Metal Oxide, Fluorescence Up-Conversion Spectroscopy, Time-Resolved Terahertz Spectroscopy, Electron Transfer

## INTRODUCTION

The direct conversion of solar power into electricity and fuels is expected to play a key role in the future development and implantation of efficient, economically viable and environmentally friendly photovoltaic and photocatalytic energy sources. Among the proposed architectures to achieve this goal, designs based on dye sensitized mesoporous metal oxides (dye-MO) represent an appealing route that has been widely scrutinized.[1-5] While quantum efficiency measurements on complete dye-MO based devices (dye-sensitized solar cells, DSSCs) enable the quantification of their global performance,[6-7] such measurements are often insufficient to disentangle the fundamental kinetical processes that might ultimately limit device efficiency.[8-11] However, the interpretation of kinetic results arising from commonly employed time-resolved spectroscopy techniques are as well complicated: many detrimental deactivation pathways after photon absorption in the sensitizer share the same fingerprint, an exponential decay, as the signal of interest (*i.e.* electron transfer from the donor to the acceptor).[11-13]

Normally, the protocol employed in pump-probe techniques for characterizing ET rates in sensitized systems realizes a comparison between the dynamics resolved on the isolated donor, and those resolved in the sensitized metal oxide. Inferring the ET from this data is achieved, in simple terms, by subtracting the rates constant from both traces.[14] While valuable, this approach assumes implicitly that the only deactivation channels activated in the donor after MO functionalization are related to favorable ET towards the acceptor. However, there are examples in the literature that challenge this view,[14] showing that other deactivation pathways are viable and measurable by the most commonly used time-resolved spectroscopy techniques.[15-18] Therefore, a quantitative assessment of the interfacial dynamics in dye-MO systems still remains as a challenging task.

A strategy to overcome the ambiguity in characterizing electron transfer in sensitized systems relies on the combination of two complementary time resolved techniques, where one technique gives access to donor dynamics and the other monitors acceptor kinetics. The validity of such an approach has been already demonstrated in dye, iron complexes and quantum dots sensitized systems.[19-23] In this work, we employ this approach by combining Fluorescence Up-Conversion Spectroscopy (FLUPS) and time resolved THz spectroscopy (TRTS) for the unambiguous characterization of ET rates and process efficiency in a sensitized interface. In contrast with former works employing transient absorption (TAS), which can provide in occasions mixed signals from both donor and acceptor in the probed frequency window,[24-25] FLUPS retrieves time-resolved emission spectra only from the molecular dye donor.[26] Therefore, we expect the combination of FLUPS and TRTS to facilitate the comparison of dynamics selectively probed in the donor and acceptor respectively. Specifically, we have employed this methodology in a model system consisting of a Coumarin 343 dye (C343) sensitizing a tin oxide ($SnO_2$) mesoporous film, an interface not previously studied under this methodology. From the characterization protocol we can unambiguously conclude that ET is biphasic in the analyzed system, *i.e.* there are no extra deactivation pathways towards the oxide electrode once it is functionalized by the dye donor.

Quantitatively, from the combination of both ultrafast methods, we resolved two ET channels that present characteristic lifetimes (and relative amplitudes) of 1.4 ± 0.1 ps (77 ± 5 %) and 17 ± 1 ps (23 ± 5 %), respectively. Thus, the combination of TRTS and FLUPS is presented here as a reliable approach for the rational characterization of sensitized systems. Hence, we believe that such methodology might contribute to a better understanding of the fundamentals of photoinduced ET in sensitized systems, leading to improved photoconversion efficiencies in related optoelectronic devices.

## METHODS

**Fabrication of the C343-$SnO_2$ film.** To fabricate the MO layer, we first prepare a $SnO_2$ paste via the sonication method as described by Cheema *et al*.[27] We then cast the $SnO_2$ paste onto a fused silica substrate by the doctor blade technique. Using a scotch tape with a known thickness (50 μm/layer), we estimate a ~0.25 mm thickness for the $SnO_2$ paste before sintering. The $SnO_2$ paste is sintered by a two-step annealing process: 1) increase from room temperature to 150ºC in 20 min, then keep the temperature for 1 hour; 2) increase from 150ºC to 600ºC in 1 hour and maintained for 2 hours (see S1~~4~~), before letting the sintered $SnO_2$ film cool to room temperature.

To obtain the dye-MO film, the $SnO_2$ films are heated again from room temperature to 150ºC in 20 min, and keep it for 1 hour and then immersed in a 0.3mM solution of C343 in a 1:1 acetonitrile:ethanol mixture. The carboxylate group of the C343 leads the anchoring of the dye to the MO. To ensure a good C343 coverage level, we keep the samples in the solution for about 20 hours. After that, the resulting C343-$SnO_2$ film is rinsed multiple times with EtOH to remove the excess unanchored dye and left to dry under a controlled air flow in a fume hood. The resulting C343-$SnO_2$ film has a 10-15 μm thickness and a surface roughness of several hundreds of nanometers (see S2).

**Fluorescence Up-Conversion Spectroscopy.** FLUPS is a convenient tool to characterize the photo-excited electron population in the dye LUMO by monitoring changes in the FL spectra when it is in competition with the ET. To time-resolve the FL, FLUPS produces a cross-correlation between the FL and gate femtosecond laser pulse, thus giving an up-converted FL spectrum with sub-ps resolution.[28] The $SnO_2$ alone is not expected to give any additional contribution to the FL since its energy gap is larger than the pump pulse (see S3). The determination of the ET rates in sensitized systems from FL is often done by subtracting the decay rates before and after MO sensitization.[14] This protocol assumes that any change in the FL is due to the introduction of an ET channel when the MO is sensitized by the dye. However, this approximation excludes the possibility that the sensitization adds new non-radiative recombination channels, such as those linked to dye aggregation,[11,29-30] which might go unnoticed or neglected. Since the temporal trace of the FL after sensitization typically follows multi-exponential decays, the employment of a FLUPS characterization alone represents a challenge for disentangling the relevant ET components from the collected data.[26]

We have carried out FLUPS measurements with a commercial spectrometer (HALCYONE, Ultrafast Systems) described elsewhere.[31] The fundamental output (100 fs and 1 mJ per pulse, λ = 800

nm, 1 kHz repetition rate) of a CPA Ti:sapphire laser (Spitfire, Spectra-Physics) is split into two beams. The first is attenuated and used as a gate ($\omega_{gate}$). This pulse goes through a double-pass delay stage, which allows a time-resolved trace on a 3 ns window with a time resolution of ~1 ps. The second beam is sent through a 1 mm slab β-barium borate crystal (BBO) for second harmonic generation (400 nm) and used as a pump ($\omega_{pump}$). This beam is then attenuated to the desired pump fluence with a variable ND filter. Then, to photoexcite the sample and induce the FL ($\omega_{FL}$), the pump beam follows two different geometries. A transmission geometry, with a tighter 49 μm diameter spot, has been preferred for the C343 in an EtOH solution. For the C343-$SnO_2$ interface a reflection geometry is used, focusing the pump on a 150 μm diameter spot (see S4). Furthermore, we have used a half-wave plate to obtain a magic angle configuration (54.7º) between the polarization of the pump and gate pulses. For both types of samples, we have filtered out the residual pump photons after the sample with a 420 nm long-pass filter. Then, the FL and the gate pulses are focused into a 0.1 mm slab BBO, where the sum frequency between the FL and the gate pulses generates the up-converted pulse ($\omega_{u\text{-}c} = \omega_{FL} + \omega_{gate}$). By means of a 15º rotation of the 0.1 mm thick BBO produced with a dc servo controller, we manage to capture all the detectable FL spectrum between 420 and 650 nm. The spectral resolution is 27 nm (250 meV at 530 nm). Finally, the up-converted pulse is focused and collected with an optical fiber, sent to a spectrograph, and the spectrum is measured with a thermoelectrically cooled CCD camera.

**Time-Resolved Terahertz Spectroscopy.** TRTS allows us to characterize the pump-induced free electrons that are injected into the MO CB and to time-resolve the photoconductivity of a system.[32-33] In our TRTS experiment, an ultraviolet pump pulse (400 nm) excites the dye, whereas a second pulse in the THz regime probes the population of free electrons in the MO CB.[34-35] Here, the dye-donor dynamics are not accessible since the photon energy of a THz pulse (~4 meV) is smaller than the energy gap in the dye. Regarding the photogenerated excitons in the MO-acceptor alone, they are not mobile enough to provide a measurable modulation of the THz radiation (see S3). While TRTS seems perfectly suited to directly determine the relevant ET processes alone, other features like phonons or localized carriers, as well as eventual donor aggregates or fragments of photo-oxidized dyes at the MO,[36-37] can give rise to an apparent pump-induced conductivity. That is, by TRTS we can eventually measure some kinetics that are not linked to the free electrons in the MO, thus revealing a THz signal that can mistakenly be attributed to an ET process.

For the TRTS measurements, we have employed a home-made setup previously described.[37] To generate the THz radiation, we have used a Ti:sapphire amplified laser (Spitfire Ace, Spectra-Physics), which provides us a central wavelength of 800 nm, ~100 fs pulse length and a 1 kHz repetition rate. A fraction of the laser output is frequency doubled using a 1 mm thick BBO crystal and serves as the optical pump pulse (400 nm). The THz radiation is generated through optical rectification in a 1 mm slab of ZnTe crystal cut along the <110> plane and detected by electro-optical sampling with a gate beam on an identical ZnTe crystal, resulting in a spectral bandwidth between 0.3 and 2.5 THz. Placing an optical chopper at 500 Hz on the pump pathway and with a lock-in detection scheme, the kinetic trace

is obtained by the differential, pump-induced changes in the transmission of the THz pulses measured from the sample, $-\Delta T(\tau,t)/T(t)$, where $\tau$ represents the pump-probe delay time and $t$ indicates the gate-THz delay time. The frequency-resolved complex photoconductivity $\Delta\sigma(\tau,\omega)$ can be retrieved by the Fourier transform of $-\Delta T(\tau,t)/T(t)$.[38] From fitting the photoconductivity data with the phenomenological Drude-Smith model, using the identity $\Delta\sigma(\tau,\omega) \propto \Delta N \cdot \Delta\mu$, we determine the photocarrier density ($N$) and the photocarrier mobility ($\mu$). According to the Drude-Smith formula, the mobility $\mu$, is given by $\mu = (e\tau/m^*)\cdot(1+c)$,[39] where $m^*$ is the effective mass of electrons in the MO and $c$ the so-called backscattering parameter.

**RESULTS AND DISCUSSION**

We start our characterization by measuring the FLUPS dynamics of C343 in solution (a 0.3mM in EOH). The employed pump wavelength was 400 nm, at a fluence of 531 μJ/cm$^2$. Under these conditions the measured dynamics represent first order processes (see S5). Figure 1a shows the recorded normalized FLUPS dynamics (black empty dots), which arise from the integrated FL in the energy range between 2.2 and 2.6 eV (Figure 1b). Fitting the FLUPS dynamics by an exponential decay function provides a lifetime of 4.0 ± 0.1 ns. We further corroborated this with the measurement of the TRPL by time-correlated single photon counting, which provided a decay lifetime of 3.86 ± 0.01 ns (see S6). Both values are in close agreement with previous reports.[40-43] However, it is worth mentioning here that the temporal FLUPS trace in our samples also revealed a fast rise kinetic component lasting about 28 ± 2 ps (see S7). This signal seems too slow to be attributed to solvent reorganization, reported to take place in the sub-ps scale.[44] Furthermore, we have purposely measured away from FLUPS magic angle condition and found that now a fast decay with the same lifetime contributes to the monitored dynamics. We suggest that this component is likely linked to an experimental artifact (see S7). In any case, whether the resolved fast kinetic component might have any eventual influence on the estimation of the ET will be clarified later.

In order to retrieve ET dynamics from FLUPS data alone, we monitor the FLUPS signal on a C343-$SnO_2$ film (Figure 1c, black empty dots; pump wavelength of 400 nm and a fluence of 181 μJ/cm$^2$). Once more, under these conditions, the measured dynamics represent first order processes (see S5). The temporal trace, which represents the integrated FLUPS contribution from 2.2 eV to 2.6 eV, as shown in Figure 1d, can be properly fitted by a function consisting of two exponential decays convoluted with the instrument response function (IRF) (see S8 and S9). From the fitting protocol, we obtained lifetimes of $\tau_{1,C343\text{-}SnO_2}$ = 1.2 ± 0.1 ps (72 ± 2 %) and $\tau_{2,C343\text{-}SnO_2}$ = 16 ± 1 ps (28 ± 2 %) (see S10). The biphasic nature of the relaxation dynamics is indeed consistent with the FLUPS spectra shown in Figure 1d, where we observe at least two peaks with different kinetic evolution over the monitored spectral bandwidth available in FLUPS (see S11, Figure S7f). Provided that the FLUPS lifetime monitored for the C343 in solution is way bigger than those monitored for the C343-$SnO_2$ film, by subtracting the decay rates of

the C343 in solution to those of the C343-$SnO_2$ film data we conclude two ET lifetimes arising from FLUPS characterization defined as $\tau_1$ = 1.2 ± 0.1 ps and $\tau_2$ = 16 ± 1 ps (see S10).

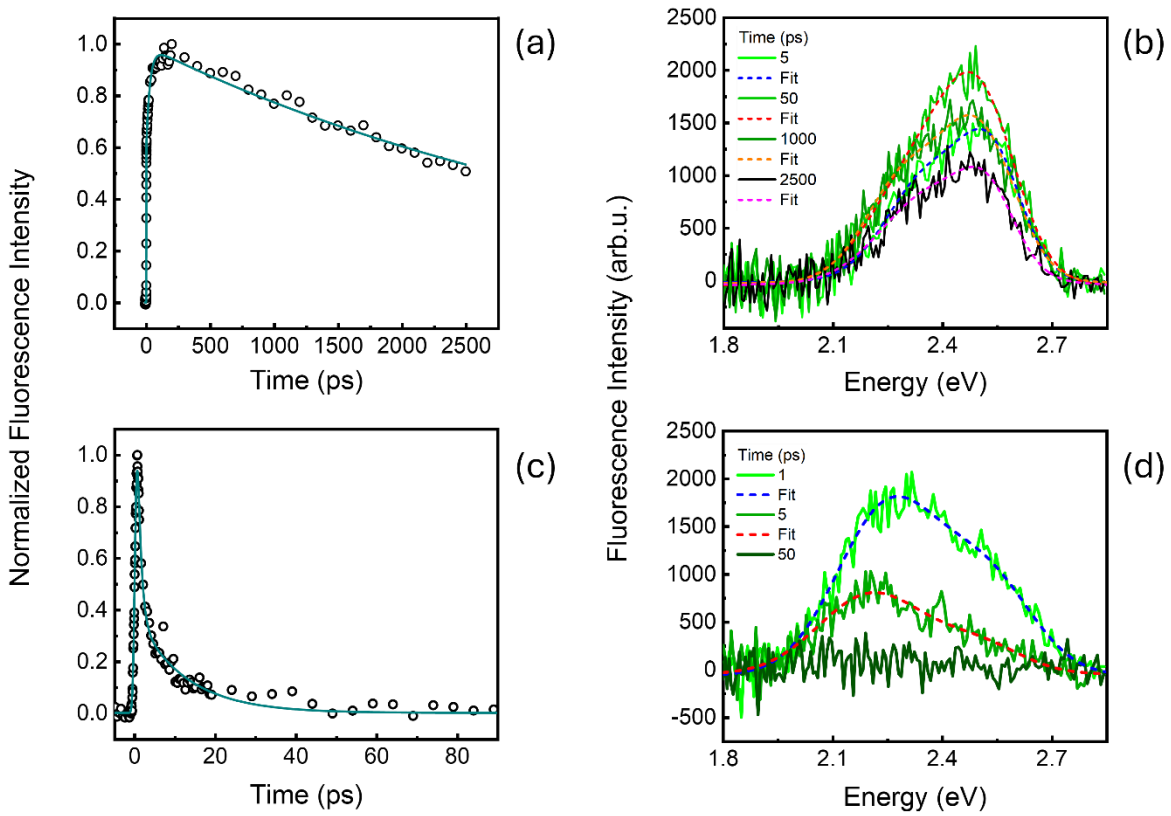


**Figure 1.** (a) Normalized intensity of the FL temporal trace from a 0.3mM C343 solution in EtOH (black empty dots) excited with a pump fluence of 531 μJ/cm$^2$. The fit curve used (teal solid line) is a convolution of a biexponential decay with a Gaussian pulse. (b) Intensity of the FL spectrum at different times for 0.3mM C343 solution in EtOH; two Gaussian function fits are depicted for the spectral trace at different times (short, dashed lines). (c) Normalized intensity of the FL temporal trace from a C343-$SnO_2$ interface (black empty dots) excited with a pump fluence of 181 μJ/cm$^2$. The fit curve used (teal solid line) is a convolution of a biexponential decay with a Gaussian pulse. (d) Intensity of the FL spectrum at different times. The up-converted FL temporal traces shown in (a) and (c) have been obtained upon spectral integration in the 2.2-2.6 eV range prior to normalization.

The observation of biphasic dynamics agrees well with a previous report on C343-$SnO_2$ film measured by Transient Absorption Spectroscopy (TAS).[45] However, we remark here that to ascertain unambiguously the nature of the biphasic components is very challenging by monitoring depopulation dynamics from the dye alone (by e.g. FLUPS or TAS). As briefly noted in the introduction, the observation of two exponential decay channels characterized after sensitizing the $SnO_2$ can indicate a variety of scenarios, e.g. two different C343-MO conformations, which might provide different interfacial energetics or coupling,[46] or one bonded dye molecule injecting towards the MO CB plus a signal related with aggregation of C343 molecules.[47-48] In this respect, from FLUPS measurements alone we can only conclude at this stage the existence of two separate deactivation channels after the

functionalization of the $SnO_2$ with the C343 dye molecule. In other words, we cannot reliably assure whether just one or perhaps both kinetic components indicate an efficient ET process. To verify whether the biphasic components resolved in FLUPS reveal or not ET processes towards the oxide electrode we performed TRTS measurements in the C343-$SnO_2$ film. We note that being TRTS primarily sensitive to the pump-induced photoconductivity of a given system, it will resolve in principle free charge carriers dynamics in the MO CB only, which is the part of the sample where a finite mobility for the charge carriers is expected. In this respect, if both kinetic pathways in FLUPS are indeed ET processes, we should resolve the same timescales by TRTS, *i.e.* when probing the arrival of charge carriers from the dye donor towards the MO acceptor.

We started the TRTS characterization by checking the response of the C343 in EtOH solution and obtained, as expected for an excitonic system, a null signal vs pump probe delay (see S12). As a second check, we also measured the TRTS signal of the bare $SnO_2$ mesoporous film, obtaining again a null photoconductivity response under the same excitation conditions employed in FLUPS (400nm, see S12). After these needed controls,[14] we monitored the TRTS dynamics in the dye-MO sensitized C343-$SnO_2$ sample (Figure 2a, black open circles, pump wavelength of 400 nm and a fluence of 424 $\mu J/cm^2$). Under these conditions the recorded dynamics are in the linear regime (see S13). As evident from the plot, right after photoexcitation, the time-resolved TRTS dynamics present a biphasic rise of the photoconductivity which is followed by a slower long-lived monophasic decay. The latter could be related with recombination at the $SnO_2$[49] and/or with back electron transfer of the injected electrons towards the dye.[50-51] The orange line in Figure 2a refers to the best fit obtained when considering a biexponential growth and a single exponential decay convoluted with the IRF of the setup (see S9 and S14). Such model has been previously used for dye-$SnO_2$ mesoporous interfaces.[24] From the fit, we obtain $\tau_1$ = 1.4 ± 0.1 ps (77 ± 3 %) and $\tau_2$ = 10 ± 2 ps (23 ± 3 %) (see S6). The monophasic long-lived decay is $\tau_{eff}$ = 660 ± 70 ps. To support that bi-exponential dynamics are linked to free carriers in the MO, we measured the frequency-resolved complex photoconductivity after the pump photoexcitation (Figure 2b). As previously resolved for mesoporous metal oxides,[49,52] the photoconductivity data from the C343-$SnO_2$ sensitized sample is well reproduced by the Drude-Smith model (see S15). This model reveals that the probed free electrons experience a certain degree of localization in the mesoporous MO. Finally, by using reported values of the effective mass $m^*$ in $SnO_2$, 0.41 ± 0.10 $m_e$,[53-54] we can infer a charge carrier mobility for the probed free electrons of $\mu$ = 150 ± 60 $cm^2V^{-1}s^{-1}$; in good agreement with the values reported for $SnO_2$ thin films, ranging between 25-130 $cm^2V^{-1}s^{-1}$.[55]

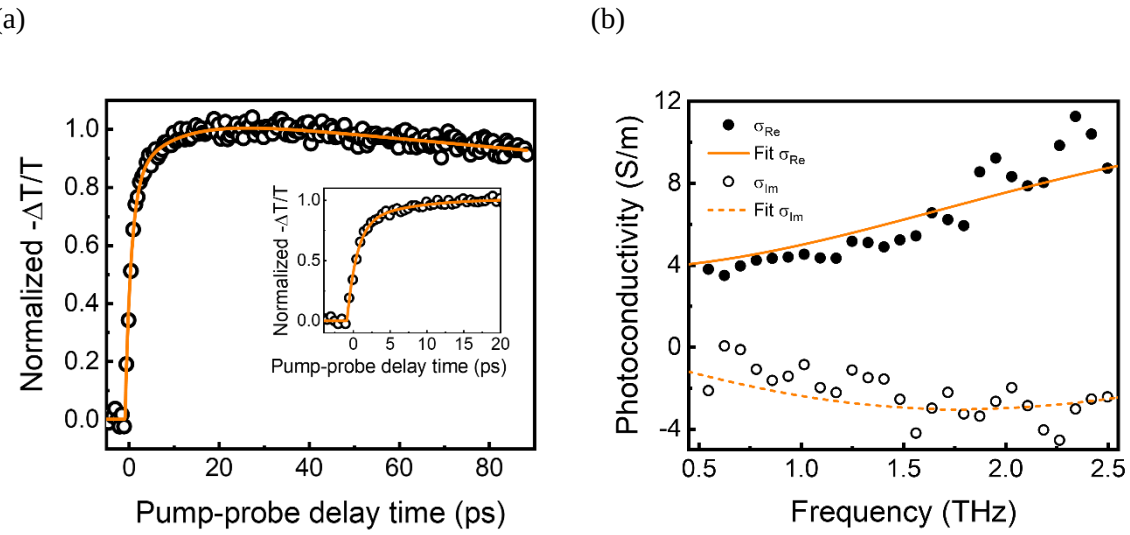


**Figure 2.** (a) Normalized differential transmission of the C343-$SnO_2$ film at a pump fluence of 424 μJ/cm$^2$ (black open circles). Fit of the temporal trace from TRTS, according to the two ET model, is depicted by orange solid line. Inset: Zoom in the first 20 ps regarding the bi-exponential increase. (b) Photoconductivity spectrum of the C343-$SnO_2$ film at 80 ps after pump photoexcitation and at a pump fluence of 490 μJ/cm$^2$. Real and imaginary components are indicated by black solid and empty circles, respectively. The Drude-Smith fitting function for the real component is indicated by orange straight line, with a dashed orange line for the imaginary component.

At this stage, we compare the lifetimes and relative amplitudes obtained independently from both methods. In FLUPS, we obtain for the slow and fast components figures of $\tau_1$ = 1.2 ± 0.1 ps (72 ± 2 %) and $\tau_2$ = 16 ± 1 ps (28 ± 2 %). For TRTS we obtain figures of $\tau_1$ = 1.4 ± 0.1 ps (77 ± 3 %) and $\tau_2$ = 10 ± 2 ps (23 ± 3 %). The agreement is almost quantitative within error, demonstrating unambiguously that two independent ET channels from the dye towards the MO are present at the sensitized interface. However, a non-negligible difference is observed in the obtained lifetimes for the slower component. We believe that this difference could arise from several sources that might even contribute in parallel: i) the finite and limited energy bandwidths of the probes for both methods, narrower in FLUPS than in steady-state measurements, and ii) the differences in probe area for both methods. Despite these issues, which will be explored in further detail in a follow-up work, the resolved correspondence of the ET lifetimes is the main result of this work. Such agreement illustrates that the combination of FLUPS and TRTS is capable to discriminate unambiguously whether monitored signals resolved independently by both methods refer or not to ET components at the sensitized interface.

As an additional way to ascertain the bi-phasic nature of the resolved ET signals, we have performed a global fit protocol to the combined data and used it as an input for the energy dependent FLUPS data. Figure 3a shows the results of the combined global fit (orange line for TRTS and red line for FLUPS), where we have assumed common ET lifetimes and independent relative contributions for the obtained kinetics in the sensitized systems. The results are summarized in Table 1 (see S16). The global fit retrieves a fast lifetime of $\tau_1$ = 1.4 ± 0.1 ps, and a slower lifetime of $\tau_2$ = 17 ± 1 ps. By employing the obtained lifetimes as fixed parameters, we have fitted globally all the temporal traces along the

bandwidth probed by FLUPS (between 2 and 2.7 eV on increments of approximately 0.07 eV) and inferred for each one the amplitudes of the corresponding time constants for each energy. Figure 3b illustrates the resulting spectral amplitudes of the $\tau_1$ and $\tau_2$ components (see S17). From the result, it is possible to see that $\tau_1$ is associated with a broad feature that peaks approximately at 2.55 eV (purple dots), while $\tau_2$ seems to originate from a contribution centered around 2.35 eV (red dots). While the centers of both peaks could be affected by the limited spectral bandwidth of FLUPS with respect to steady-state measurements (see Methods), the shape of the spectrum gives further support to the scenario where we consider that two ET channels are operative in the sensitized samples. Furthermore, from this global fit we can conclude that these two ET channels are related with two, non-interacting donating populations of C343 sensitizing the $SnO_2$ surface. Note that, if the populations of both donating states were correlated, *e.g.* via energy transfer or a vibrational relaxation of the dye excited state, the spectral amplitude of one state would be anticorrelated with the second one.

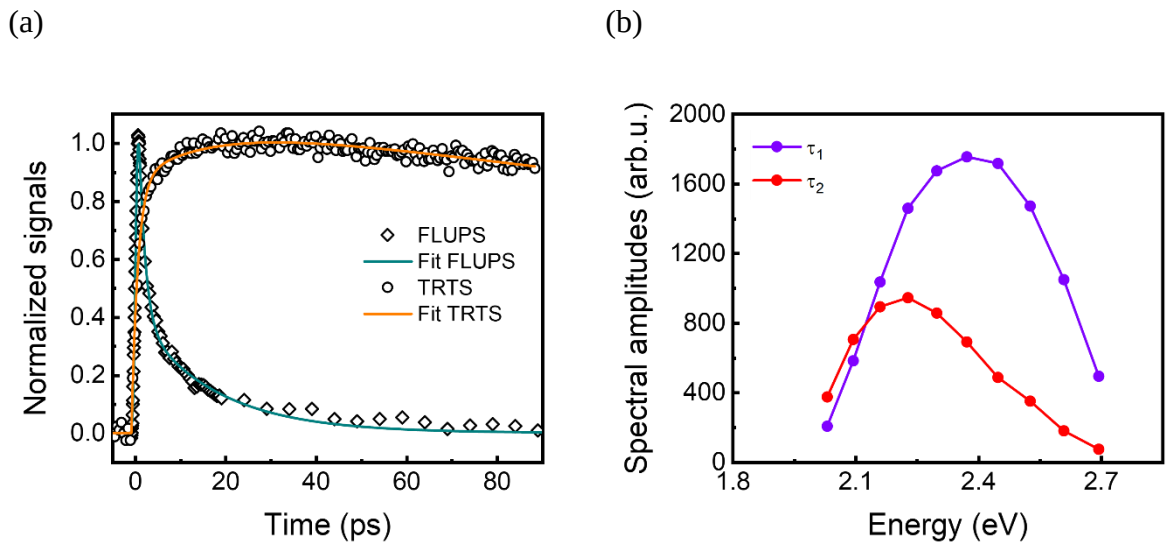


**Figure 3.** (a) Global fit analysis of the temporal traces from FLUPS and TRTS on the C343-$SnO_2$ interface. The temporal trace from FLUPS is the averaged between 2.2 and 2.6 eV at a pump fluence of 191 μJ/cm$^2$, whereas the temporal trace from TRTS is obtained at a pump fluence of 424 μJ/cm$^2$. The teal and orange lines are the fitting curves for FLUPS and TRTS data, respectively. (b) Global fit analysis on the spectral amplitudes of the ET lifetimes obtained with the first global fit: $\tau_1$, 1.38 ± 0.07 ps, and $\tau_2$, 17 ± 1 ps.

| | **Parameter** | **Fitted value** |
|---|---|---|
| Shared lifetimes (ps) | $\tau_1$ | 1.4 ± 0.1 |
| | $\tau_2$ | 17 ± 1 |
| **FLUPS** | $A_1$ (%) | 72.5 ± 0.9 |
| | $A_2$ (%) | 27.5 ± 0.9 |
| **TRTS** | $A_1$ (%) | 78 ± 5 |
| | $A_2$ (%) | 22 ± 5 |

Table 1. Resume of lifetimes and their relative amplitudes values from the global fit of TRTS and FLUPS on C343-$SnO_2$ film.

## CONCLUSIONS

In summary, we have demonstrated the feasibility and potential of combining FLUPS and TRTS to address unambiguously the biphasic nature of ET in a C343-$SnO_2$ dye-sensitized mesoporous oxide film. Where the two donating states are independent of each other, *i.e.* non-interacting. Thus, the combination of TRTS and FLUPS reveals a reliable avenue for the rational characterization of sensitized systems. We expect this approach will contribute to a better understanding of photo-induced dynamics in these technologically relevant interfaces. Particularly, we believe that the employed approach might shed light on resolving the kinetic fingerprint of deactivation channels linked to trap states in the MO and/or to the presence of donor aggregates, two aspects that certainly have been reported in literature to compromise the efficiency on complete devices. Furthermore, we see a clear potential to employ the combination of FLUPS and TRTS with other sensitizers, specifically with quantum dots (QD), where deactivation channels competing with ET and linked to trapping at the QD surface could be most likely ubiquitous among the samples reported in most of the literature.

## ▪ ASSOCIATED CONTENT

### Supporting Information

The Supporting Information is available free of charge via the internet at (…)

C343-$SnO_2$ sample preparation, Profilometer and atomic force microscopy (AFM) measurements on a C343-$SnO_2$ film, C343 and $SnO_2$ energy levels alignment, Pump diameter in FLUPS transmission and reflection measurements, Pump fluence dependence measurements in FLUPS, Time-Resolved Photoluminescence (TRPL) measurement of C343 in solution, Fast lifetime in FLUPS measurement of C343 in solution, Dynamic model in presence of two ET channels, Equations of two ET model for fitting FLUPS and TRTS data, Relative amplitudes of lifetimes and ET lifetimes in FLUPS and TRTS, Comparison of steady-state PL and FLUPS measurements, TRTS measurements of $SnO_2$ film and C343 in solution, Pump fluence dependence measurements in TRTS, Comparison of one and two electron transfer models fitting TRTS data, Drude-Smith model for frequency-resolved complex photoconductivity, First global fit, Second global fit.

## ▪ AUTHOR INFORMATION


### Corresponding Author

**Enrique Cánovas** – *Instituto Madrileño de Estudios Avanzados en Nanociencia (IMDEA Nanociencia), Calle Faraday 9, 28049 Madrid, Spain. E-mail:* enrique.canovas@imdea.org

### Authors

**Miguel Ángel Pulido-Lendínez** – *Instituto Madrileño de Estudios Avanzados en Nanociencia (IMDEA Nanociencia), Calle Faraday 9, 28049 Madrid, Spain.*

**Marco Ballabio** – *Instituto Madrileño de Estudios Avanzados en Nanociencia (IMDEA Nanociencia), Calle Faraday 9, 28049 Madrid, Spain.*

**Andrés Burgos-Caminal** – *Instituto Madrileño de Estudios Avanzados en Nanociencia (IMDEA Nanociencia), Calle Faraday 9, 28049 Madrid, Spain.*
*Departamento de Química, Facultad de Ciencias, Universidad Autónoma de Madrid, Calle Francisco Tomás y Valiente 7, 28049 Madrid, Spain.*

**María E. Corrales** –*Departamento de Química, Facultad de Ciencias, Universidad Autónoma de Madrid, Calle Francisco Tomás y Valiente 7, 28049 Madrid, Spain.*
*Departamento de Química Física Aplicada, Facultad de Ciencias, Universidad Autónoma de Madrid, Calle Francisco Tomás y Valiente 9, 28049 Madrid, Spain*

**Sergio Revuelta** – *Instituto Madrileño de Estudios Avanzados en Nanociencia (IMDEA Nanociencia), Calle Faraday 9, 28049 Madrid, Spain.*

**Saül Garcia-Orrit** – *Instituto Madrileño de Estudios Avanzados en Nanociencia (IMDEA Nanociencia), Calle Faraday 9, 28049 Madrid, Spain.*

**Víctor Vega-Mayoral** – *Instituto Madrileño de Estudios Avanzados en Nanociencia (IMDEA Nanociencia), Calle Faraday 9, 28049 Madrid, Spain.*

**Juan Cabanillas-González** – *Instituto Madrileño de Estudios Avanzados en Nanociencia (IMDEA Nanociencia), Calle Faraday 9, 28049 Madrid, Spain.*

**Luis Bañares** – *Instituto Madrileño de Estudios Avanzados en Nanociencia (IMDEA Nanociencia), Calle Faraday 9, 28049 Madrid, Spain.*
*Departamento de Química Física, Facultad de Ciencias Químicas, Universidad Complutense de Madrid, Plaza de las Ciencias 2, 28040 Madrid, Spain.*
*Center for Ultrafast Lasers (CLUR), Facultad de Ciencias Químicas, Universidad Complutense de Madrid, Plaza de las Ciencias 2, 28040 Madrid, Spain.*

**Wojciech Gawelda** – *Instituto Madrileño de Estudios Avanzados en Nanociencia (IMDEA Nanociencia), Calle Faraday 9, 28049 Madrid, Spain.*
*Departamento de Química, Facultad de Ciencias, Universidad Autónoma de Madrid, Calle Francisco Tomás y Valiente 7, 28049 Madrid, Spain.*

**Notes**

The authors declare no competing financial interests.

## ▪ ACKNOWLEDGMENTS

E.C. acknowledges funding from Spanish MICIU through Proyecto de I+D+i 2019 PDI2019-107808RA-I00 and CNS2022-136203 - Consolidación investigadora. E.C. also acknowledge financial support from the Comunidad de Madrid through Projects No. 2017-T1/AMB-5207 and No. 2021–5A/AMB-20942.

V.V.-M. acknowledges grant TED2021-131906A-100, funded by Spanish Ministry of Science, Innovation and Universities (10.13039/501100011033) and support from the Regional Government of Madrid through a Talento's grant (2019-T2/IND-12737).

L.B. acknowledges the support provided by the Spanish Ministry of Science, Innovation and Universities (MICIU) under grant PID2021-122839NB-I00.

W.G. further acknowledges the funding from Spanish MIU through "*Ayudas Beatriz Galindo*" (BEAGAL18/00092), Comunidad de Madrid and Universidad Autónoma de Madrid through Proyecto de I+D para Investigadores del Programa Beatriz Galindo (SI2/PBG/2020-00003), Spanish MICIU through Proyecto de I+D+i 2019 (PID2019-108678GB-I00) and Proyecto de I+D+i 2022 (PID2022-140257NB-I00).

M.A.P.L and S.G.-O thanks the funding provided from the FPI fellowship PRE2020-094744 and PRE2019-09345.

M.B thanks the funding received from the grant JDC2022-048249-I funded by MICIU/AEI/10.13039/501100011033 and by the "European Union NextGenerationEU/PRTR".

A.B.-C is funded by the IDEAL project, receiving funding from the European Union's Horizon 2020 research and innovation programme under the Marie Skłodowska-Curie grant agreement No. 101034431. We acknowledge financial support from the "Severo Ochoa" Programme for Centers of Excellence in R&D (CEX2020-001039S / AEI / 10.13039/501100011033). We also acknowledge the assistance of Dr. Reinhold Wannemacher in the TCSPC measurements, Manuel Rodríguez for the profilometer measurements, and Patricia López for the AFM measurements.

## ▪ REFERENCES

(1) B. O'Regan, M. Grätzel, "A low-cost, high-efficiency solar cell based on dye-sensitized colloidal $TiO_2$ films", *Nature* **353**, 737-740 (1991), https://doi.org/10.1038/353737a0

(2) O. I. Francis, and A. Ikenna, "Review of Dye-Sensitized Solar Cell (DSSCs) Development", *Natural Science*, 13(12), 496-509 (December 2021), https://doi.org/10.4236/ns.2021.1312043

(3) J. Gong, K. Sumathy, Q. Qiao, and Z. Zhou, "Review on dye-sensitized solar cells (DSSCs): Advanced techniques and research trends", *Renewable and Sustainable Energy Reviews*, 68 (2017), 234-246, https://doi.org/10.1016/j.rser.2016.09.097

(4) M. L. Parisi, S. Maranghi, R. Basosi, "The evolution of the dye sensitized solar cells from Grätzel prototype to up-scaled solar applications: A life cycle assessment approach", *Renewable and*

*Sustainable Energy Reviews*, volume 39, 2014, pages 124-138, ISSN 1364-0321, https://doi.org/10.1016/j.rser.2014.07.079

(5) Md. K. Nazeeruddin, E. Baranoff, M. Grätzel, "Dye-sensitized solar cells: A brief overview", *Solar Energy*, volume 85, Issue 6, 2011, pages 1172-1178, ISSN 0038-092X, https://doi.org/10.1016/j.solener.2011.01.018

(6) K. Sharma, V. Sharma, and S. S. Sharma, "Dye-Sensitized Solar Cells: Fundamental and Current Status", *Nanoscale. Res. Lett.* **13**, 381 (2018), https://doi.org/10.1186/s11671-018-2760-6

(7) K. Hara, K. Sayama, Y. Ohga, A. Shinpo, S. Suga, and H. Arakawa, "A coumarin-derivative dye sensitized nanocrystalline $TiO_2$ solar cell having a high solar-energy conversion efficiency up to 5.6%", *Chem. Commun.*, 2001, 569-570, https://doi.org/10.1039/B010058G

(8) B. C. O'Regan, and J. R. Durrant, "Kinetic and Energetic Paradigms for Dye-Sensitized Solar Cells: Moving from the Ideal to the Real", *Acc. Chem. Res.* 2009, 42, 11, 1799-1808, https://doi.org/10.1021/ar900145z

(9) G. Boschloo, "Improving the Performance of Dye-Sensitized Solar Cells", *Front. Chem.* 2019; 7:77, https://doi.org/10.3389/fchem.2019.00077

(10) J. V. S. Krishna, N. V. Krishna, T. H. Chowdhury, S. Singh, I. Bedja, A. Islam, and L. Giribabu, "Kinetics of dye regeneration in liquid electrolyte unveils efficiency of 10.5% in dye-sensitized solar cells", *J. Mater. Chem. C*, 2018, **6**, 11444-11456, https://doi.org/10.1039/C8TC04370A

(11) C. Martín, M. Ziółek, and A. Douhal, "Ultrafast and fast charge separation processes in real dye-sensitized solar cells", *Journal of Photochemistry and Photobiology C: Photochemistry Reviews*, volume 26, 2016, pages 1-30, ISSN 1389-5567, https://doi.org/10.1016/j.jphotochemrev.2015.12.001

(12) A. Listorti, B. O'Regan, and J. R. Durrant, "Electron Transfer Dynamics in Dye-Sensitized Solar Cells", *Chem. Mater*. 2011, 23, 15, 3381-3399, https://doi.org/10.1021/cm200651e

(13) J. R. Durrant, S. A. Haque, and E. Palomares, "Towards optimisation of electron transfer processes in dye sensitized solar cells", *Coordination Chemistry Reviews*, Volume 248, Issues 13-14, 2004, 1247-1257, https://doi.org/10.1016/j.ccr.2004.03.014

(14) M. Ballabio, and E. Cánovas, "Electron Transfer at Quantum Dot-Metal Oxides Interfaces for Solar Energy Conversion", *ACS Nanoscience Au* 2022, 2, 5, 367-395, https://doi.org/10.1021/acsnanoscienceau.2c00015

(15) Y. Tachibana, J. E. Moser, M. Grätzel, D. R. Klug, and J. R. Durrant, "Subpicosecond Interfacial Charge Separation in Dye-Sensitized Nanocrystalline Titanium Dioxide Films", *J. Phys. Chem.* 1996, 100, 51, 20056-20062, https://doi.org/10.1021/jp962227f

(16) S. E. Koops, and J. R. Durrant, "Transient emission studies of electron injection in dye sensitised solar cells", *Inorganica Chimica Acta*, Volume 361, Issue 3, 2008, 663-670, https://doi.org/10.1016/j.ica.2007.05.021

(17) P. Tiwana, P. Docampo, M. B. Johnston, H. J. Snaith, and L. M. Herz, “Electron Mobility and Injection Dynamics in Mesoporous ZnO, $SnO_2$, and $TiO_2$ Films Used in Dye-Sensitized Solar Cells”, *ACS Nano*, 2011, 5, 6, 5158-5166, https://doi.org/10.1021/nn201243y

(18) J. J. H. Pijpers, R. Ulbricht, S. Derossi, J. N. H. Reek, and M. Bonn, “Picosecond Electron Injection Dynamics in Dye-Sensitized Oxides in the Presence of Electrolyte”, *J. Phys. Chem. C* 2011, 115, 5, 2578-2584, https://doi.org/10.1021/jp1104246

(19) D. Zigmantas, T. Polívka, P. Persson, and V. Sundström, “Ultrafast laser spectroscopy uncovers mechanisms of light energy conversion in photosynthesis and sustainable energy materials”, *Chem. Phys. Rev.* 3, 041303 (2022), https://doi.org/10.1063/5.0092864

(20) H. Němec, P. Kužel, V. Sundström, “Charge transport in nanostructured materials for solar energy conversion studied by time-resolved terahertz spectroscopy”, *Journal of Photochemistry and Photobiology A: Chemistry*, 215 (2010), 123-139, https://doi.org/10.1016/j.jphotochem.2010.08.006

(21) J. C. Brauer, A. Marchioro, A. A. Paraecattil, A. A. Oskouei, and J.-E. Moser, “Dynamics of Interfacial Charge Transfer States and Carriers Separation in Dye-Sensitized Solar Cells: A Time-Resolved Terahertz Spectroscopy Study”, *J. Phys. Chem. C* 2015, 119, 47, 26266-26274, https://doi.org/10.1021/acs.jpcc.5b06911

(22) T. C. B. Harlang, Y. Liu, O. Gordivska, L. A. Fredin, C. S. Ponseca Jr., P. Huang, P. Chábera, K. S. Kjaer, H. Mateos, J. Uhlig *et al*., “Iron sensitizer converts light to electrons with 92% yield”, *Nature Chemistry*, 7, 883-889 (2015), https://doi.org/10.1038/nchem.2365

(23) K. Žídek, K. Zheng, C. S. Ponseca Jr., M. E. Messing, L. R. Wallenberg, P. Chábera, M. Abdellah, V. Sundström, and T. Pullerits, “Electron Transfer in Quantum-Dot-Sensitized ZnO Nanowires: Ultrafast Time-Resolved Absorption and Terahertz Study”, *J. Am. Chem. Soc.* 2012, 134, 29, 12110-12117, https://doi.org/10.1021/ja3029679

(24) M. Juazapavicius, M. Kaucikas, S. D. Dimitrov, P. R. F. Barnes, J. J. van Thor, and B. C. O’Regan, “Evidence for “Slow” Electron Injection in Commercially Relevant Dye-Sensitized Solar Cells by vis-NIR and IR Pump-Probe Spectroscopy”, *J. Phys. Chem. C* 2013, 117, 48, 25317-25324, https://doi.org/10.1021/jp408989q

(25) A. Glinka, J. Kubicki, and M. Ziółek, “Complexity of Electorn Injection Dynamics and Light Soaking Effects in Efficient Dyes for Modern DSSC”, *Energies* 2021, *14*(2), 407, https://doi.org/10.3390/en14020407

(26) Jianhua Xu, and Jay R. Knutson, “Ultrafast Fluorescence Spectroscopy via Upconversion: Applications to Biophysics”, *Methods in Enzymology*, Vol. 450, 159-183 (2008), https://doi.org/10.1016/S0076-6879(08)03408-3

(27) H. Cheema, and J. H. Delcamp, “$SnO_2$ Transparent Printing Pastes from Powders for Photon Conversion in $SnO_2$ Based Dye-Sensitized Solar Cells”, *Chem. Eur. J.* **2019**,25(62), 14205-14213, https://doi.org/10.1002/chem.201903292

(28) H. Chosrowjan, S. Taniguchi, and F. Tanaka, “Ultrafast fluorescence upconversion technique and its applications to proteins”, *FEBS Journal* **282** (2015), 3003-3015, https://doi.org/10.1111/febs.13180

(29) D. Lee, L. Greenman, M. Sarovar, and K. B. Whaley, “Ab Initio Calculation of Molecular Aggregation Effects: A Coumarin-343 Case Study”, *J. Phys. Chem A* 2013, 117, 43, 11072-11085, https://doi.org/10.1021/jp405152h

(30) X. Liu, J. M. Cole, and K. S. Low, “Molecular Origins of Dye Aggregation and Complex Formation Effects in Coumarin 343”, *J. Phys. Chem. C* 2013, 117, 28, 14723-14730, https://doi.org/10.1021/jp4024266

(31) C. Sun, L. Bai, J. C. Roldao, A. Burgos-Caminal, O. Borrel-Grueiro, J. Lin, W. Huang, J. Gierschner, W. Gawelda, L. Bañares *et al*., “Boosting the Stimulated Emission Properties of Host:Guest Polymer Blends by Inserting Chain Twists in the Host Polymer”, *Adv. Funct. Mater*. **2022**, 32(48), 2206723, https://doi.org/10.1002/adfm.202206723

(32) R. Ulbricht, E. Hendry, J. Shan, T. F. Heinz, and M. Bonn, “Carrier dynamics in semiconductors studied with time-resolved terahertz spectroscopy”, *Rev. Mod. Phys.* **2011**, *83*, 543, https://doi.org/10.1103/RevModPhys.83.543

(33) C. A. Schmuttenmaer, “Exploring Dynamics in the Far-Infrared with Terahertz Spectroscopy”, *Chem. Rev*. **2004**, 104, 4, 1759-1780, https://doi.org/10.1021/cr020685g

(34) H. Němec, P. Kuzěl, V. Sundström, “Charge transport in nanostructured materials for solar energy conversion studied by time-resolved terahertz spectroscopy”, *Journal of Photochemistry and Photobiology A: Chemistry*, 215(2-3), 2010, 123-139, https://doi.org/10.1016/j.jphotochem.2010.08.006

(35) H. Němec, J. Rochford, O. Taratula, E. Galoppini, P. Kužel, T. Polívka, A. Yartsev, and V. Sundström, “Influence of the Electron-Cation Interaction on Electron Mobility in Dye-Sensitized ZnO and $TiO_2$ Nanocrystals: A Study Using Ultrafast Terahertz Spectroscopy”, *Phys. Rev. Lett*. 2010, 14;104(19):197401, https://doi.org/10.1103/PhysRevLett.104.197401

(36) E. Cánovas, P. Moll, S. A. Jensen, Y. Gao, A. J. Houtepen, L. D. A. Siebbeles, S. Kinge, and M. Bonn, “Size-Dependent Electron Transfer from PbSe Quantum Dots to $SnO_2$ Monitored by Picosecond Terahertz Spectroscopy”, *Nano Lett.* 2011, 11, 5234-5239, https://doi.org/10.1021/nl202550v

(37) M. Karakus, W. Zhang, H. J. Räder, M. Bonn, and E. Cánovas, “Electron Transfer from Bi-Isonicotinic Acid Emerges upon Photodegradation of N3-Sensitized $TiO_2$ Electrodes”, *ACS. Appl. Mater. Interfaces*, 2017, 9, 35376-35382, https://pubs.acs.org/doi/full/10.1021/acsami.7b08986

(38) S. Revuelta, and E. Cánovas, “Exciton formation dynamics at the $SiO_2$/Si interface”, *Commun. Mater*. **4**, 97 (2023), https://doi.org/10.1038/s43246-023-00427-7

(39) X. Zou, J. Luo, D. Lee, C. Cheng, D. Springer, S. K. Nair, S. A. Cheong, H. J. Fan, and E. E.M. Chia, "Temperature-dependent terahertz conductivity of tin oxide nanowire films", *J. Phys. D: Appl. Phys.* **45** (2012), 465101 (6pp), https://doi.org/10.1088/0022-3727/45/465101

(40) H.-M. Tsai, J. S. Souris, H.-J. Kim, S.-H. Cheng, L. Chen, L.-W. Lo, C.-T. Chen, and C.-M. Kao, "Note: Rapid measurement of fluorescence lifetimes using SiPM detection and waveform sampling", *Rev. Sci. Instrum.* 88(9): 096107 (2017), https://doi.org/10.1063/1.5003413

(41) K. Hara, T. Sato, R. Katoh, A. Furube, Y. Ohga, A. Shinpo, S. Suga, K. Sayama, H. Sugihara, and H. Arakawa, "Molecular Design of Coumarin Dyes for Efficient Dye-Sensitized Solar Cells", *J. Phys. Chem. B* 2003, 107, 2, 597-606, https://doi.org/10.1021/jp026963x

(42) D. Pant, and H. H. Girault, "Time-resolved total internal reflection fluorescence spectroscopy. Part I. Photophysics of Coumarin 343 at liquid/liquid interface", *Phys. Chem. Chem. Phys.*, 2005, **7**, 3457-3463, https://doi.org/10.1039/B507830J

(43) M. M. LaRocca, G. A. Baker, and M. P. Heitz, "Assessing rotation and solvation dynamics in ethaline deep eutectic solvent and its solution with methanol", *J. Chem. Phys.* **155**, 034505 (2021), https://doi.org/10.1063/5.0056653

(44) G. C. Walker, W. Jarzeba, T. J. Kang, A. E. Johnson, and P. F. Barbara, "Ultraviolet femtosecond fluorescence spectroscopy: techniques and applications", *J. Opt. Soc. Am. B* 7, 1521-1527 (1990), https://doi.org/10.1364/JOSAB.7.001521

(45) D. Stockwell, Y. Yang, J. Huang, C. Anfuso, Z. Huang, and T. Lian, "Comparison of Electron-Transfer Dynamics from Coumarin 343 to $TiO_2$, $SnO_2$, and ZnO Nanocrystalline Thin Films: Role of Interface-Bound Charge-Separated Pairs", *J. Phys. Chem C* 2010, 114, 14, 6560-6566, https://doi.org/10.1021/jp912133r

(46) W. Wu, Z. Cao, Y. Zhao, "Theoretical studies on absorption, emission, and resonance Raman spectra of Coumarin 343 isomers", *J. Chem. Phys.* 136, 114305 (2012), https://doi.org/10.1063/1.3693264

(47) D. Lee, L. Greenman, M. Sarovar, and K. B. Whaley, "Ab Initio Calculation of Molecular Aggregation Effects: A Coumarin-343 Case Study", *J. Phys. Chem A* 2013, 117, 43, 11072-11085, https://doi.org/10.1021/jp405152h

(48) X. Liu, J. M. Cole, and K. S. Low, "Molecular Origins of Dye Aggregation and Complex Formation Effects in Coumarin 343", *J. Phys. Chem. C* 2013, 117, 28, 14723-14730, https://doi.org/10.1021/jp4024266

(49) K. P. Regan, J. R. Swierk, J. Neu, and C. A. Schmuttenmaer, "Frequency-Dependent Terahertz Transient Photoconductivity of Mesoporous $SnO_2$ Films", *J. Phys. Chem. C* 2017, 121, 29, 15949-15956, https://doi.org/10.1021/acs.jpcc.7b02318

(50) D. Liu, W. Fesseden, G. L. Hug, and P. V. Kamat, "Dye Capped Semiconductor Nanoclusters. Role of Back Electron Transfer in the Photosensitization of $SnO_2$ Nanocrystallites with Cresyl Violet Aggregates", *J. Phys. Chem. B* 1997, 101, 14, 2583-2590, https://doi.org/10.1021/jp962695p

(51) L. Troian-Gautier, R. N. Sampaio, E. J. Piechota, M. D. Brady, and G. J. Meyer, "Barriers for interfacial back-electron transfer: A comparison between $TiO_2$ and $SnO_2/TiO_2$ core/shell structures", *J. Chem. Phys.* **150**, 041719 (2019), https://doi.org/10.1063/1.5054604

(52) E. Cinquanta, E. A. A. Pogna, L. Gatto, S. Stagira, and C. Vozzi, "Charge carrier dynamics in 2D materials probed by ultrafast THz spectroscopy" (2023), *Advances in Physics: X*, 8:1, 2120416, https://doi.org/10.1080/23746149.2022.2120416

(53) G. Sanon, R. Rup, and A. Mansingh, "Band-gap narrowing and band structure in degenerate tin oxide ($SnO_2$) films", *Phys. Rev. B* **44**, 11, pp. 5672-5680, https://doi.org/10.1103/PhysRevB.44.5672

(54) M. Nagasawa, S. Shionoya, and S. Makishima, "Electron Effective Mass of $SnO_2$", *J. Phys. Soc. Jpn.* **20**, pp. 1093-1093 (1965), https://doi.org/10.1143/JPSJ.20.1093

(55) Z. Li, P. Graziosi, and N. Neophytou, "Electron and Hole Mobility of $SnO_2$ from Full-Band Electron-Phonon and Ionized Impurity Scattering Computations", *Crystals* **2022**, *12*, 1591, https://doi.org/10.3390/cryst12111591

- **TOC IMAGE**